PHYSICAL REVIEW B VOLUME 19, NUMBER 8 15 APRIL 1979

Theory of metallic adhesion

John Ferrante
National Aeronautics and Space Administration, Lewis Research Center, Cleveland, Ohio 44135

John R. Smith
Physics Department, General Motors Research Laboratories, Warren, Michigan 48090
(Received 16 October 1978)

The self-consistent electronic structure and adhesive energies are computed for the following contacts: Al(111)-Al(111); Mg(0001)-Mg(0001); Zn(0001)-Zn(0001); Na(110)-Na(110). Electronic charge densities and potentials are quite sensitive to small separations in the contacts. Friedel oscillation amplitudes increase with decreasing average bulk electron densities and with increasing separation in the contact. The inclusion of nonlocal effects increases adhesive binding energies but has little effect on the shape of the adhesive energy versus separation plots. The importance of bulk equilibrium is investigated. Binding energies agree well with experimental surface energies and very good agreement is found between computed elastic constants and experiment. Both the binding energies and the elastic constants increase with increasing average bulk-electron number density. The variation of the components of the adhesive energy with separation reveal a rather close analogy between the characteristics of the metallic adhesive bond and those of molecular bonds in simple molcules. The kinetic energy initiates the bond, while the electrostatic and particularly the exchange energy lead to the strong adhesive bond. The range of the strong bonding is about 0.2 nm. Adhesive energies and charge densities saturate much faster with contact separation than do electronic potentials.

I. INTRODUCTION

The strong adhesive bond formed between metal surfaces in intimate contact plays an important role in deposition of metal films, grain boundary energetics, friction and wear, and fracture. There has been considerable experimental work in the field of metallic adhesion, as discussed recently in the reviews of Tabor[1] and Buckley.[2]

The first basic physical theory[3] of the strong short-range interaction at bimetallic interfaces was done for contacts between the close-packed surfaces of Al, Mg, and Zn. The Hohenberg and Kohn[4] (HK) formalism was used to evaluate total energies as a function of interface separation. Simple overlap of the metal-vacuum charge distributions was used. The exchange energy was shown to be quite important to the binding. It was found that registry effects at the interface between crystalline planes also contributed significantly. Some insight into the mechanisms of metallic transfer at the interface was obtained. The range of the strong bonding was shown to be about 0.2 nm.

Allan *et al.*[5] employed a semiempirical technique to estimate the dependence of interface energies on such properties as d-band filling. Inglesfield[6] improved upon the gradient-expansion[4] kinetic-energy expression and obtained adhesive energies for Al. Interface energies for interacting jellia were computed recently by Mehrotra *et al.*,[7] Muscat and Allan,[8] and Swingler and Inkson.[9] The importance of crystallinity in the adhesive bond between metals was recently demonstrated by Smith and Ferrante.[10]

Some authors have concentrated on electronic properties such as charge densities and barrier heights, rather than adhesive energies or forces. Bennett and Duke[11] made the first serious calculation of interface electronic structure. They solved the Kohn-Sham[12] equations for jellium interfaces with only partial self-consistency.[13] Swingler and Inkson[14] solved the same problem using a linearized Thomas-Fermi expression including nonlocal exchange. Yaniv[15] used a tight-binding technique to determine how interface densities of states vary with surface parameters.

Full self-consistency was first introduced into metallic interface electronic structure and adhesive energy calculations by Ferrante and Smith.[16] The Kohn-Sham equations were solved self-consistently for an Al(111)-Al(111) contact. The electron density distributions and barrier heights were found to be strong functions of interface separation.[17-19] The minimum in the adhesive-binding-energy curve occurred at an interplanar separation that was within 0.01 nm of the experimental bulk spacing. The binding energy at the minimum, or the surface energy, agreed reasonably well with experiment.

In the following we report results of fully self-consistent calculations of adhesive energies for interfaces between[20] Zn(0001)-Zn(0001), Mg(0001)-Mg(0001), and Na(110)-Na(110), as well as Al(111)-

Al(111). The effect of nonlocality in the exchange and correlation energies is investigated. Adhesive energies, forces, charge densities, and potentials are reported as a function of contact separation. The effect of bulk equilibrium on the binding-energy curves is also exhibited. Computed binding energies and elastic-stiffness constants are compared with experiment. The energy components (kinetic, electrostatic, etc.) of the adhesive bond are computed as a function of contact separation. A strong parallel with molecular bonding is evidenced.

II. THEORETICAL METHODS

The calculational formalism methods used for obtaining self-consistent interface electronic structure will now be presented. A much more extensive description is given in Ref. 21, particularly of numerical techniques.

The adhesive interaction energy, E_{ad}, between two metal surfaces is a function of the distance between the two surfaces, a (see Fig. 1). E_{ad} is defined as the negative of the amount of work necessary to increase the separation from a to ∞ divided by twice the cross-sectional area A. Thus

$$E_{ad} = [E(a) - E(\infty)]/2A \,, \tag{1}$$

where E is the total energy. For identical metals, E_{ad} is the negative of the surface energy when a is at the energy minimum (Figs. 4 and 5).

According to the density functional formalism of Hohenberg, Kohn, and Sham,[4,12] the total energy is given by (atomic units are used throughout unless otherwise specified)

$$E\{n(\vec{r})\} = \int v(\vec{r}) n(\vec{r})\, d\vec{r} + \frac{1}{2} \sum_{i \neq j} \frac{z_i z_j}{R_{ij}} + F\{n(\vec{r})\} \,, \tag{2}$$

where

$$F\{n(\vec{r})\} = T_s\{n(\vec{r})\} + \frac{1}{2} \iint \frac{n(\vec{r}) n(\vec{r}')}{|\vec{r} - \vec{r}'|}\, d\vec{r}\, d\vec{r}' + E_{xc}\{n(\vec{r})\} \,, \tag{3}$$

$v(\vec{r})$ is the ionic potential, and $n(\vec{r})$ is the electron number density. The first two terms in Eq. (2) are the electron-ion and ion-ion interaction energies, respectively. z is the ionic charge and R_{ij} is the distance between ion core nuclei (there is no ion core overlap in the systems considered here). $T_s\{n(\vec{r})\}$ is the kinetic energy of a system of noninteracting electrons with the same density $n(\vec{r})$, the next term is the classical electron-electron interaction energy, and E_{xc} is the exchange-correlation energy.

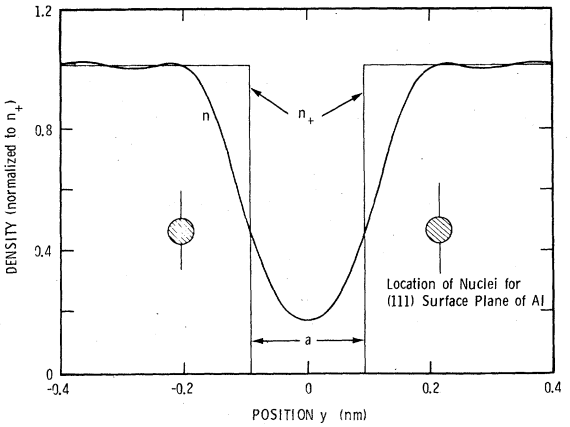

FIG. 1. Electron number density n and jellium ion charge density n_+ for Al-Al contact normalized to unit density.

For metals like Zn, Mg, Al, and Na, the jellium model (Fig. 1) is a good zeroth-order approximation, and the difference between the total pseudopotential and the potential due to the jellium is small for the closest packed plane. Thus for a given separation a, one obtains E to a first-order perturbation approximation as[22,23]

$$E\{n(\vec{r})\} = A \int v_J(y,a) n(y,a)\, dy + \frac{1}{2} \sum\sum_{i \neq j} \frac{z_i z_j}{R_{ij}} + F\{n(y,a)\} + A \int \delta v(y,a) n(y,a)\, dy \,, \tag{4}$$

where v_J is the potential produced by the jellium, y is the direction normal to the surfaces, and δv is the average, over planes parallel to the surface, of the difference in potential between an array of pseudopotentials and the jellium. Following Lang and Kohn[24,25] the Ashcroft pseudopotential is used:

$$v_{ps}(r) = \begin{cases} 0, & r \leq r_c \\ -z/r, & r > r_c, \end{cases} \tag{5}$$

where r_c is determined empirically[26] and is close to the ion core radius.

The electron number density is obtained from a set of self-consistent equations of the form

$$\left(-\frac{1}{2}\frac{d^2}{dy^2} + v_{eff}(n;y)\right)\psi_k^{(i)}(y) = \tfrac{1}{2}(k^2 - k_F^2)\psi_k^{(i)}(y) \,,$$

$$n(y,a) = \frac{1}{4\pi^2} \sum_{i=1}^{2} \int_0^{k_F} dk\, |\psi_k^{(i)}(y)|^2 (k_F^2 - k^2) \,, \tag{6}$$

$$v_{eff}(n;y) = \phi(y,a) + \frac{\delta E_{xc}\{n(y,a)\}}{\delta n(y,a)} \,,$$

with Poisson's equation

$$\frac{d^2\phi(y,a)}{dy^2} = -4\pi[n(y,a) - n_+(y)]. \quad (7)$$

$\phi(y,a)$ is the electrostatic potential energy, $\psi_k^{(i)}(y)$ is a doubly degenerate wave function ($i=1,2$), k_F is the Fermi-wave-vector magnitude, and $n_+(y)$ is the jellium density (Fig. 1).

It is useful to combine the first two terms of Eq. (4) along with the classical electron-electron interaction term of $F\{n(y,a)\}$ as follows:

$$-\tfrac{1}{2}A\int \rho(y,a)\phi(y,a)\,dy + W_{\text{int}}, \quad (8)$$

where $\rho(y,a)$ is the net charge density of the zeroth-order or jellium solution. W_{int} is the exact difference between the ion-ion and the jellium-jellium interaction. It is shown in Ref. 3 that W_{int}/A is negligible unless the facing planes are in registry, i.e., commensurate. Full expressions for W_{int}/A as a function of separation a are given in Ref. 3 for fcc (111) planes and in Appendix A for hcp (0001) and bcc (110) planes. Also highly accurate, simple analytic approximations to W_{int}/A are presented.

There is a close analogy between adhesive energy calculations and cohesive energy and elastic constant calculations. W_{int} is an interface analog of the Ewald energy. The rest of the terms in Eq. (4) are analogous to the structure independent cohesive energy terms of Eq. (4.6) of Ref. 27. There is one important difference, however. In cohesion and elastic constant calculations, the electron density is often taken to be uniform prior to perturbation by the ion cores. In our adhesion calculations, the unperturbed electron density varies with the coordinate perpendicular to the surface, as in Fig. 1. Because of that, we will see that there is also an analogy with molecular binding. Further, the accuracy of computations of elastic stiffness constants associated with the direction perpendicular to the interface is improved by allowing variation of the unperturbed electron density in that direction.

The exchange-correlation energy E_{xc} is often written in the local-density approximation (LDA),

$$E_{xc}\{n(\vec{r})\} = \int n(\vec{r})\epsilon_{xc}(n(\vec{r}))\,d\vec{r}\,, \quad (9)$$

where $\epsilon_{xc}(n(\vec{r}))$ is the exchange-correlation energy of a uniform electron gas of number density $n(\vec{r})$. We use[3] Wigner's interpolation formula for the correlation energy.

There have been a number of workers who have recently provided or used expressions for $E_{xc}\{(n(\vec{r})\}$ beyond the LDA at metal surfaces.[28-32] Lau and Kohn[29] were the first to include gradient terms in $E_{xc}\{n(\vec{r})\}$ in a surface-energy calculation:

$$E_{xc}\{n(\vec{r})\} = \int n(\vec{r})\epsilon_{xc}(n(\vec{r}))\,d\vec{r} + \frac{1}{2}\int g(n(\vec{r}))[\vec{\nabla}n(\vec{r})]^2\,d\vec{r}\,. \quad (10)$$

A function $g(n(\vec{r}))$ was derived in Ref. 29 from the static dielectric function of Vashista and Singwi.[33] Rose *et al.*[30] used a $g(n(\vec{r}))$ which was derived by Geldart and Rasolt[28] using the random phase approximation to compute surface energies. Rose *et al.*[30] obtained gradient term corrections to the surface energy (computed for $a=0$) which are in good agreement with those obtained by Lau and Kohn.[29] Gupta and Singwi[31] have computed a $g(n(\vec{r}))$ which is very close to but somewhat smaller than (within ~30%) that derived in Refs. 28 and 29. It is perhaps significant that such close agreement is obtained between two very different approaches (Refs. 28 and 31). Further, Gupta and Singwi report the next higher gradient term and state that it is much smaller than their first gradient term, thus supporting the usage of only the first gradient term.

In the next section we will present results for the first nonlocal, self-consistent adhesive energy calculation. Equation (10) is used in conjunction with Eqs. (6). The form of $g(n(\vec{r}))$ is

$$g(n(\vec{r})) = 2C(r_s(n))/n^{4/3}(\vec{r})\,, \quad (11)$$

where the $C(r_s(n))$ as provided by Geldart and Rasolt[28,34] is used [$r_s(n)$ is defined by $(4\pi/3)r_s^3(n) = 1/n(\vec{r})$].

It remains to specify the kinetic-energy functional of Eq. (3):

$$T_s\{n(y,a)\} = A\int t_s\{n(y,a)\}\,dy\,, \quad (12)$$

where

$$t_s\{n(y,a)\} = \sum_{i=1}^{2}\sum_{\substack{k,k_x,k_z\\(\text{occ.})}}(k^2+k_x^2+k_z^2)|\psi_k^{(i)}(y)|^2 + [v_{\text{eff}}(n;\pm\infty) - v_{\text{eff}}(n;y)]n(y,a)\,. \quad (13)$$

The sum is over all occupied states. When faced with the problem of evaluating $T_s\{n(y,\infty)\} - T_s\{n(y,0)\}$ for a surface energy computation, Huntington[35,36] chose to integrate first over all direct space (y). The resultant difference is between total kinetic energies, which are very large numbers. The expression he derived was used in all the modern surface energy computations (see, e.g., Refs. 23 and 24). For the adhesive energy calculation, we find a different approach to be more useful. In Appendix B, we derive an expression for $T_s\{n(y,a)\} - T_s\{n(y,0)\}$ which is based on kinetic-energy densities in the interface region. We find this approach more natural for our prob-

lem, as it is the interface region in which the large changes in kinetic energy density occur upon adhesion.

The Hamiltonian is now completely specified. In the remainder of this section we will elucidate some of the techniques used to deal with Eqs. (6) and (7).

The numerical integration of the Schrödinger equation and Poisson's equation was done over a slab whose width (distance between symmetry point and matching point to the bulk) ranged between 15 a.u. at $a = 0.25$ a.u. and 27.5 a.u. at $a = 15$ a.u. The solution of the Schrödinger equation proceeded by assuming the form of the wave function for the transmitted wave for an electron incident from the left half space to be e^{iky} deep in the bulk of the right half space.[37] The integration proceeded into the bulk of the left half space, where numerical solutions were matched to

$$\psi_k(y) = C(e^{iky} + De^{-iky}) \ . \tag{14}$$

The potential was required to be the bulk potential at the matching point.

The self-consistent solution of Eqs. (6) and (7) was obtained by means of iteration. The starting potential for $a = 0.25$ a.u. was constructed from simple overlap of metal-vacuum densities[3] with a Gaussian well which simulated the first Friedel oscillation in the potential. The iteration proceeded by means of the usual convergence factor methods. Charge neutrality was obtained by multiplication of the electron number density by a constant at each iteration. It was found that the neutralization procedure was not necessary when close to self-consistency. At completion of the iterations, the difference between input and output potentials was less than 10 meV everywhere for all separations between all metals treated. For subsequent separations, the starting potential was obtained from the self-consistent potential at the previous separation. First, the potential at the previous separation was fixed relative to the jellium surface, and then the points needed to complete the potential between the two metals were obtained by a linear extrapolation.

III. RESULTS

We now give results for the self-consistent electronic structure and binding energies for a range of separations in the following contacts: Al(111)-Al(111); Zn(0001)-Zn(0001); Mg(0001)-Mg(0001), and Na(110)-Na(110). To test first the self-consistency of the solution of Eqs. (6) and (7), one can use the Budd-Vannimenus[19] (BV) theorem. This theorem relates the jellium force at zero separation ($a = 0$) to the pressure. The jellium force can be determined from the difference in electrostatic potential between a point in the bulk and a point on the jellium surface when a is large (we took $a = 15$ a.u.). The pressure can be determined from bulk jellium properties. The results are given in Table I. One can see that the forces as determined from the bulk pressure (BV theorem) are in excellent agreement with the forces determined from the electrostatic potential difference for both the LDA and the nonlocal [see Eqs. (10) and (11)] calculations. This is an indication of the high degree of self-consistency obtained.

TABLE I. Jellium force at zero separation.

Metal	r_s	Force (a.u.) BV theorem	LDA	Nonlocal
Al	2.07	2.558×10^{-3}	2.558×10^{-3}	2.580×10^{-3}
Zn	2.30	1.365×10^{-3}	1.368×10^{-3}	1.363×10^{-3}
Mg	2.65	5.612×10^{-4}	5.615×10^{-4}	5.628×10^{-4}
Na	3.99	1.437×10^{-5}	1.452×10^{-5}	1.447×10^{-5}

Figure 2 shows the electronic charge densities $n(y)$, for three representative separations in the Na contact. Note first how sensitive $n(y)$ is to separation. For a separation of only 0.013 (0.25 a.u.), there is a significant dip in $n(y)$. This dip at the symmetry point grows rapidly with separation a, $n(y)$ being less than half n_+ at $y = 0$ for a separation of 0.16 nm (3 a.u.). At $a = 0.79$ nm (15 a.u.), the charge-density overlap between the two pieces of metal is nearly zero. We will see that this rapid variation of interaction with separation is also reflected in the adhesive energy (Fig. 4). If we compare Fig. 1 for the Al contact at $a = 0.19$ nm with the Na results of Fig. 2, we see much stronger Friedel oscillations in Na than in Al. In general, we found the Friedel oscillation amplitude to increase with increasing r_s. A similar behavior was first noted by Lang and Kohn[24] for the solid-vacuum interface. Finally, it is clear from Fig. 2 that the Friedel oscillation amplitude increases with separation, a result that was also seen earlier[16] for the Al contact. Plots of $n(y)$ as obtained

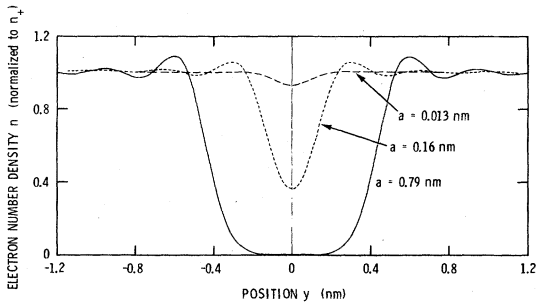

FIG. 2. Electron density vs position for a Na(011) – Na(011) contact for separations of 0.013, 0.016, and 0.79 nm.

from the nonlocal calculation were not included, because differences between them and the LDA densities were not perceptible on the scale of these plots. Complete listings of these densities are given in Ref. 21, however.

The electronic potential energies $v_{\text{eff}}(y)$ are plotted in Fig. 3 for the Na contact at the same three separations used in Fig. 2. Again the sensitivity to separation is evident with the barrier height at the symmetry point rising rapidly with separation. A similar sensitive behavior of barrier height was exhibited earlier[16] for Al, and in fact is typical of all four metals considered. Most of the electrons must tunnel between the two metals even when a is as small as 0.16 nm. While the barrier height is well above the Fermi level for $a = 0.79$ nm, there is some evidence of electronic interaction as shown in Fig. 3. That is, the obvious flattening out around $y = 0$ for $a = 0.79$ nm of the electron number density (Fig. 2) and adhesive energy (Fig. 4) is not as evident in the electronic potential energy. We found, in fact, that the electronic barrier height is still increasing slightly at $a = 0.79$ nm, enough so that we cannot estimate the work function accurately by extrapolation. It is not surprising that the adhesive energy has saturated long before the electronic potential energy. The electrostatic potential as determined from Eq. (7) is sensitive to small changes in $n(y)$. Because of the stationary property of $E\{n(\vec{r})\}$, the adhesive energy is, however, not sensitive to small changes in the electron density.[3] Note finally that, as with $n(y)$, the Friedel oscillation amplitude increases with separation for the potential energy.

Figure 4 shows the adhesive energies as a function of separation for the four crystalline metals. These curves are a surface analog of cohesive energy versus lattice constants plots for bulk materials. Results obtained using both the local and nonlocal exchange-correlation potentials are shown. Note first that all systems are bound, and that there is a minimum near $a = 0$. This minimum would occur exactly at zero if the bulk densities used (listed in Table I and taken from Ref. 24) were consistent with the Hamiltonian we use. We will deal directly with this point later in this section. We showed earlier (see Fig. 2, Ref. 10) that including the effects of crystallinity is extremely important to the shape and magnitude of these curves. Note that the range of strong bonding, i.e., that range over which the slope of the curves in Fig. 4 remains large, is about 0.2 nm. This is roughly the interplanar spacing in the bulk for these close packed planes.

Nonlocal terms do not strongly affect the shapes of the binding energy curves. They do make the adhesive binding somewhat larger in every case, however. This improves the agreement of the binding energy, as measured from the minimum, with the experimental surface energies[38-40] as shown in Fig. 4. The agreement is rather good, considering the approximations involved and the difficulty of the experiments. The poorest agreement is for Zn(0001). Monnier and Perdew[23] discovered an apparent inaccuracy in the Zn pseudopotential based on bulk calculations. Note that the binding energies or surface energies increase with decreasing r_s, or with increasing bulk average electron number density. We will find a similar correlation for elastic stiffness constants. This is not inconsistent with the fact that it is the electrons that provide the "glue" to hold the solids together. Let us speak further about the experimental data chosen. Surface-energy experiments are often performed of necessity at elevated temperatures and on liquid metals. Surface contamination and other effects can make the results of these difficult experiments questionable.[41] Our

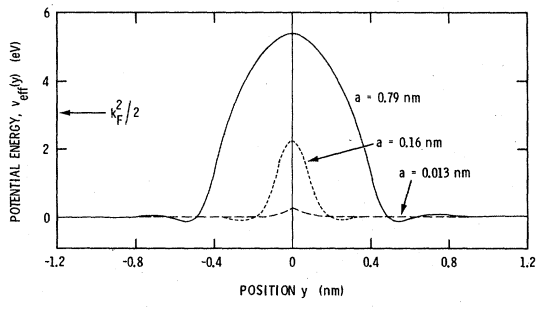

FIG. 3. Electron potential energy $v_{\text{eff}}(x)$ vs position for a Na(011)-Na(011) contact at separations of 0.013, 0.16, and 0.79 nm.

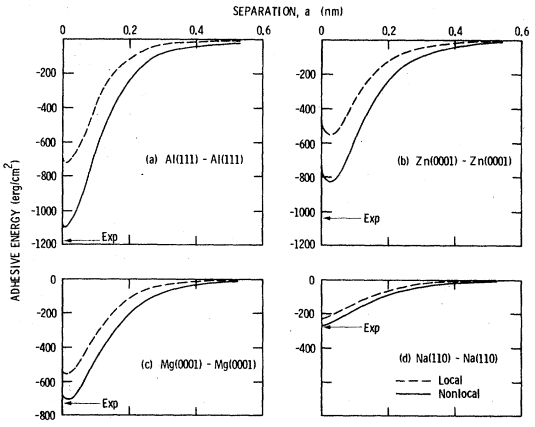

FIG. 4. Adhesive binding energy vs separation a for LDA and including nonlocal terms in the exchange and correlation energy. The experimental values refer to measured surface energies (see Refs. 38–40).

theoretical results describe brittle fracture at 0 K. Consequently it is important to obtain surface-energy data for solids at very low temperatures. Wawra[39] has determined surface energies indirectly for solids at close to 0 K by using ultrasonic attenuation. Unfortunately he has reported no data for Mg, and for that metal we were forced to extrapolate from liquid-metal data. We should mention that while the theory is for single-crystal interfaces, the experimental data do not take the grain orientation of the surface into consideration.

Inglesfield[42] has shown that for separations greater than about 0.3 nm, the Van der Waal's interaction predominates. However, he found that for separations $\lesssim 0.25$ nm, the wave functions overlap appreciably and the bonding energy is more accurately described by the exchange-correlation (LDA) expression used here.

The fact that the minimum in the curves of Fig. 4 does not occur at $a=0$ was pointed out earlier in this section. The reason for this is that the bulk solid is slightly "spring loaded". That is, the bulk lattice constants used[24] are not exactly consistent with the Kohn-Sham[12] Hamiltonian and the Ashcroft[26] pseudopotentials. To verify this, we did a bulk calculation using the same pseudopotentials and the same Hamiltonian, determining the cohesive energy as a function of bulk-lattice constant. We then determined the values of the bulk-lattice constants that minimized the cohesive energy. In the case of the hcp metals, the axial ratio that minimized the Ewald energy was used. The difference between it and the ideal ratio is negligible in the present calculation, however. The resultant values of r_s are (compare with Table I): Al, $r_s=2.10$; Zn, $r_s=2.61$; Mg, $r_s=2.79$; and Na, $r_s=3.88$. The binding energy curves computed for these equilibrium lattice constants are shown in Fig. 5. We see that in every case the expected result is obtained. That is, the position of the minimum has moved closer to zero separation. Note that the Al(111), Zn(0001), and Mg(0001) curves have effectively moved to the left, whereas the Na(110) curve has effectively moved to the right. It is as if the origins were moved to the minima of the plots of Fig. 4. The change of shape of the curves is nearly imperceptible.

Adhesive forces can be determined simply by differentiating the adhesive energy curves of Fig. 4 with respect to the separation a. We show the adhesive force for the representative case of the Mg(0001)-Mg(0001) contact in Fig. 6. The force is of course zero at the minimum in the adhesive energy plot (Fig. 4). It rises rapidly and forms a maximum at about 0.1 nm. This maximum value is the force for brittle fracture, although it is somewhat academic since plastic flow is important

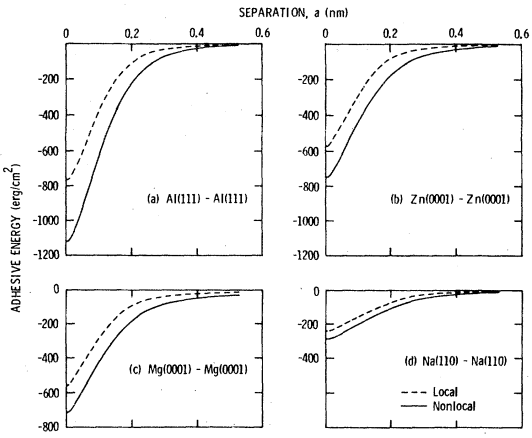

FIG. 5. Adhesive binding energy vs separation using bulk densities obtained by minimizing the cohesive energy.

in the breaking of Mg at most temperatures. The force has fallen significantly by $a=0.2$ nm, which is an effective strong bonding range which we mentioned earlier. The nonlocal approximation gives a higher maximum force in agreement with Fig. 4.

Note that the rise in the force near $a=0$ is nearly linear up to about one-half the maximum value. From the slope, one can approximate the elastic stiffness constant[43] associated with the direction perpendicular to the interface, $C_{\parallel}'$:

$$\frac{C_{\parallel}'}{d} \simeq \left.\frac{d^2E(a)}{da^2}\right|_{a_0} . \tag{15}$$

a_0 is the separation at the binding energy minimum and d is the interplanar spacing. $C_{\parallel}'$ is otherwise known as a uniaxial strain modulus. Equation (15) is shown as an approximation because in our adhesion calculation only the planes just at the interface have their spacing changed, the near-neighbor spacing between the other planes remaining fixed. In the measurement of elastic constants an

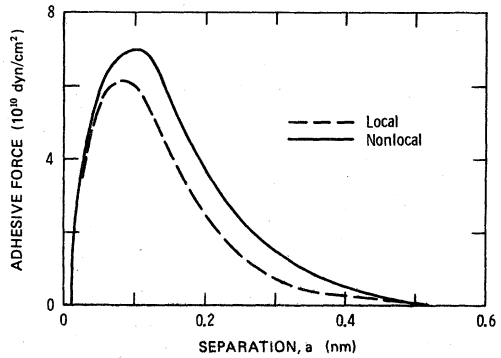

FIG. 6. Adhesive force vs separation for a Mg(0001) – Mg(0001) contact for the LDA and including nonlocal terms in the exchange and correlation energies.

TABLE II. Elastic stiffness constant $C_{\|}'(10^{12}$ dyn/cm^2).

	Theory		
	Local	Nonlocal	Experiment
Al(111)	0.746	1.23	1.23[a]
Zn(0001)	0.680	0.927	0.688[b]
Mg(0001)	0.619	0.666	0.665[c]
Na(110)	0.183	0.170	0.133[d]

[a] Reference 46.
[b] Reference 47.
[c] Reference 48.
[d] Reference 49.

ultrasonic pulse method[43,44] is often used. The wavelength is of the order of 3×10^{-2} cm, many interplanar spacings. However, the approximation is not too severe because Tyson[45] has pointed out that in most bcc metals the forces become quite small beyond second-nearest-neighbor atoms (planes) and, for fcc crystals, they are quite small beyond first near neighbors. This is presumably because of the ability of metals to screen perturbations over a short range. As mentioned in the previous section, the accuracy of our computations of $C_{\|}'$ is enhanced by allowing the electron gas to relax as the spacing is increased. Because of that, our results for $C_{\|}'$ are more accurate than what one would expect from a first-order perturbation-theory calculation done for bulk metals. In terms of phonon dispersion relations, our "nearest-neighbor" approximation is equivalent to

$$\omega^2(q) \propto C_{\|}'(1-\cos qd)\,, \tag{16}$$

where q is the wave vector.

The results for $C_{\|}'$ as computed from Eq. (15) are shown in Table II. Also included are experimental values. Note first that the magnitude of the stiffness constants increases with average bulk electron number density, as did the surface energies. Also there is rather good agreement between theory and experiment, particularly for the case of the nonlocal values. The agreement is perhaps better than one should expect, considering our approximations. The inclusion of nonlocal effects improved the agreement with experiment for every case but Zn(0001). Zn(0001) exhibited the largest error in the surface energy and, as mentioned earlier, Monnier and Perdew[23] found the Zn pseudopotential to be relatively inaccurate. Na(110) had the most accurate surface energy, whereas its computed elastic constant is not the most accurate. Second nearest neighbors, as Tyson[45] notes, may be relatively more important for the bcc metal Na than for the other metals.[50-53]

One of the basic physical questions that we would like to answer is what is the nature of the "glue" which holds these metal interfaces together, and is there an anlalogy with molecular bonding. In Fig. 7 is a plot of the energy components versus separation for the Mg(0001)-Mg(0001) interface. The total energy curve (dashed) is the same as the LDA plot from Fig. 4. At large separations, the kinetic energy component is attractive, while the electrostatic energy is repulsive. Thus the kinetic energy initiates the bond between the metals. This behavior is paralleled in molecular bonding,[54,55] even for a molecule as simple as H_2. There it is argued[54] that the kinetic energy decrease results from a smoothing of the wave functions as the orbitals of the two species begin to overlap. The potential energy increase presumably results from an increase in the electron density between the species due to this overlap. This pulls electrons from the vicinity of the nuclei (where the potential energy is large and negative), thereby increasing the electrostatic term. As the metals push closer together, the kinetic energy rises and becomes the repulsive term. The electrostatic energy becomes attractive. The dominant attractive term, however, is the exchange-correlation energy. It is this exchange-correlation energy that solidifies the strong bond that forms between metal surfaces. The increase in the kinetic energy at small separations arises qualitatively from orbital contraction. The lowering of the electrostatic energy at small separation can be thought of as coming from electrons being pushed into the vicinity of the nuclei. These kinetic and electrostatic energy effects have been thoroughly discussed[54,55] in terms of simple, prototype molecules. Thus there is a strong analogy between molecular bonding and bonding between metal surfaces.

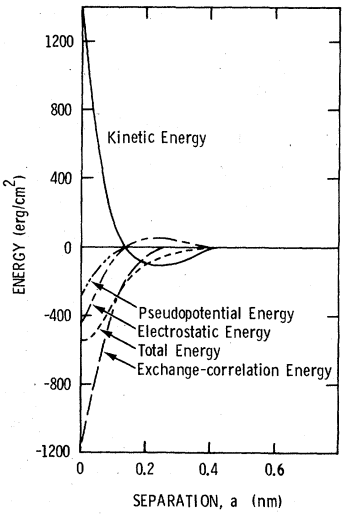

FIG. 7. Self-consistent energy components of the binding energy for a Mg(0001) – Mg(0001) contact. The electrostatic energy is given by Eq. (8) and the pseudopotential energy is the last term in Eq. (4).

IV. SUMMARY

We see that there is a close analogy between molecular bonding and adhesive bonding between metals. The kinetic energy initiates the bond, and the electrostatic energy and particularly the electron exchange energy form the strong bond. The range of the strong bonding is about 0.2 nm, which is roughly the bulk interplanar spacing. Nonlocal effects increase the binding energies, but have little effect on the shape of the binding energy versus separation plots. There is good agreement between experimental surface energies and theoretical binding energies. Elastic stiffness constants were computed and very good agreement with experiment was found. Both binding energies and elastic stiffness constants increase with average bulk electron densities. It was found that the bulk was slightly "spring loaded." That leads to an adhesive energy minimum that falls at a point that is not located exactly at the bulk interplanar spacing. Electronic charge densities and potentials are very sensitive to separation between metal surfaces. Friedel oscillation amplitudes in charge densities and potentials increase with r_s (decreasing average bulk electron density) and with separation between metals. Adhesive energies and electronic charge densities saturate much faster with separation than do electronic potential energies.

ACKNOWLEDGMENTS

The authors would like to thank J. C. Tracy, S. V. Pepper, R. A. Ayres, P. L. Taylor, D. H. Buckley, and R. H. Wagoner for useful comments on various aspects of this work.

APPENDIX A: EXPRESSIONS FOR $W_{\rm int}(a)$

$W_{\rm int}$ is introduced in Eq. (8), and is the difference between the classical ion-ion and jellium-jellium interactions. It is an interface analog of the Ewald electrostatic energy.

An exact expression for $W_{\rm int}(a)$ is derived in Ref. 3 for fcc (111) planes. The following approximate expression was also derived in Ref. 3 for perfect registry between hcp(0001)-hcp(0001) or fcc(111)-fcc(111):

$$\frac{W_{\rm int}(a)}{A} = -\frac{2\sqrt{3}z^2}{c^3}\exp\left(\frac{-2\pi}{c}\frac{2}{\sqrt{3}}(d+a)\right), \quad \text{(A.1)}$$

where d is the distance between planes parallel to the surface in the metal and c is the distance between near neighbors in a given lattice plane. It was shown in Ref. 3 that (A.1) is rather accurate (see Table I) for Al(111)-Al(111).

The following is a similarly derived expression for bcc(110)-bcc(110):

$$\frac{W_{\rm int}(a)}{A} = \frac{3\sqrt{6}z^2}{4c^3}\left[\tfrac{1}{2}\exp\left(\frac{-2\pi\sqrt{2}}{c}(d+a)\right) - \frac{2\pi}{\sqrt{3}}\exp\left(\frac{-2\pi}{c}\sqrt{\frac{3}{2}}(d+a)\right)\right]. \quad \text{(A.2)}$$

One can also derive exact expressions for hcp(0001)-hcp(0001) and bcc(110)-bcc(110) using a technique analogous to that used in Ref. 3 for fcc(111)-fcc(111):

hcp(0001)

$$\frac{W_{\rm int}}{A} = 4\beta z n_+ \sum_{m=1}^{\infty}(m-1)\left[\sum_{h=1}^{\infty}\frac{1+\cos\pi h}{h}\sqrt{3}X^{-2mh/\sqrt{3}}X^{-ah/\sqrt{3}d}\left(\cos\frac{2\pi h}{3}+2X^{2h/\sqrt{3}}+X^{h/\sqrt{3}}\cos\frac{2\pi h}{3}\right)\right.$$
$$+\sum_{l=1}^{\infty}\frac{1+\cos\pi l}{l}X^{-2ml}X^{-al/d}(X^{3l}+2X^{2l}+X^{l})$$
$$\left.+\sum_{l=1}^{\infty}\sum_{h=1}^{\infty}\frac{2[1+\cos\pi(h+l)]}{D}X^{-2mD}X^{-aD/d}\left(X^{3D}\cos\frac{2\pi h}{3}+2X^{2D}+X^{D}\cos\frac{2\pi h}{3}\right)\right], \quad \text{(A.3)}$$

where $\beta \equiv \sqrt{3}\,d/45c$, $D \equiv \sqrt{l^2+\frac{1}{3}h^2}$, and $X \equiv \exp(2\pi d/c)$.

bcc(110)

$$\frac{W_{\rm int}}{A} = zn_+\sum_{m=1}^{\infty}(m-1)\left(\sum_{h=1}^{\infty}\frac{1+\cos\pi h}{h}\frac{\sqrt{2}}{2}X^{-\sqrt{2}mh}X^{-ah/\sqrt{2}d}(X^{3h\sqrt{2}}+2X^{\sqrt{2}h}\cos\pi h+X^{h/\sqrt{2}})\cos\pi h\right.$$
$$+\sum_{l=1}^{\infty}\frac{1+\cos\pi l}{2l}X^{-2ml}X^{-a/dl}(X^{3l}+2X^{2l}+X^{l})$$
$$\left.+\sum_{l=1}^{\infty}\sum_{h=1}^{\infty}\frac{1+\cos\pi(h+l)}{B}X^{-2mB}X^{-aB/d}(X^{3B}+2X^{2B}\cos\pi h+X^{B})\cos\pi h\right), \quad \text{(A.4)}$$

where $B \equiv \sqrt{l^2+\frac{1}{2}h^2}$.

APPENDIX B: KINETIC ENERGY

It is desired to provide an expression for $E_k(a)$, where

$$E_k(a) \equiv T_s\{n(y,a)\} - T_s\{n(y,0)\}. \tag{B.1}$$

The kinetic energy contribution to E_{ad} is then given by Eq. (1) as

$$[E_k(a) - E_k(\infty)]/2A\ . \tag{B.2}$$

The general expression for $T_s\{n(y,a)\}$ is given in Eqs. (12) and (13). Now

$$E_k(a) = 2A\int_{-\infty}^{0} [t_s\{n(y,a)\} - \tfrac{3}{10}(3\pi^2)^{2/3} n_+^{5/3}(y)]\,dy\ . \tag{B.3}$$

In evaluating $E_k(a)$, we must deal with the sums in Eq. (13). Let us take the repeat distances in the x and z directions to be L_x and L_z, respectively. The wave numbers k_x and k_z have the forms $2\pi m_x/L_x$ and $2\pi m_z/L_z$, respectively. If we take the thickness of the film for $a=0$ to be $2L$, then the sum over states in $\vec{k}$ space becomes (see, e.g., Ref. 36):

$$\sum_{k,k_x,k_z} \rightarrow \frac{L_x L_z L}{(2\pi)^3}\left[1 + O\left(\frac{1}{L}\right)\right]\int dk\,dk_x\,dk_z\ . \tag{B.4}$$

Thus to $O(1/L)$,

$$t_s\{n(y,a)\} = \frac{L}{16\pi^2}\sum_{i=1}^{2}\int_0^{k_F} dk\,|\psi_k^{(i)}(y)|^2(k_F^2 - k^2)(k^2 + k_F^2) + [v_{\text{eff}}(n;\pm\infty) - v_{\text{eff}}(n;y)]n(y;a)\ . \tag{B.5}$$

Since

$$t_s\{n(y,a)\} \xrightarrow[y\to\pm\infty]{} \tfrac{3}{10}(3\pi^2)^{2/3} n_+^{5/3}\ , \tag{B.6}$$

$$E_k(a) \cong 2A\int_{-y_0}^{0} [t_s\{n(y,a)\} - \tfrac{3}{10}(3\pi^2)^{2/3} n_+^{5/3}(y)]\,dy\ , \tag{B.7}$$

where y_0 is chosen large enough to obtain the desired accuracy. y_0 values ranged from 15 to 27.5 a.u., the larger values used with larger a values. We could check our values of $E_k(a)$ for $a=\infty$ with the results Lang and Kohn[24] obtained for integral r_s values. Generally excellent agreement was found. Similarly excellent agreement for Al, Zn, Mg, and Na at $a=\infty$ was found with the results of Monnier and Perdew.[23]

[1] D. Tabor, in *Surface Physics of Materials*, edited by J. M. Blakely (Academic, New York, 1975), Chap. 10, Vol. 2.
[2] D. H. Buckley, J. Colloids Interface Sci. 58, 36 (1977).
[3] John Ferrante and J. R. Smith, Surf. Sci. 38, 77 (1973).
[4] P. Hohenberg and W. Kohn, Phys. Rev. 136, B864 (1964).
[5] G. Allan, M. Lannoo, and L. Dobrzynski, Philos. Mag. 30, 33 (1974).
[6] J. E. Inglesfield, J. Phys. F 6, 687 (1976).
[7] R. Mehrotra, M. M. Pant, and M. P. Das, Solid State Commun. 18, 199 (1976).
[8] J. P. Muscat and G. Allan, J. Phys. F 7, 999 (1977).
[9] J. N. Swingler and J. C. Inkson, Solid State Commun. 24, 305 (1977).
[10] J. R. Smith and John Ferrante, Solid State Commun. 21, 1059 (1976).
[11] Alan J. Bennett and C. B. Duke, Phys. Rev. 160, 541 (1967); 162, 578 (1967).
[12] W. Kohn and L. J. Sham, Phys. Rev. 140, A1133 (1965).
[13] J. Heinrichs and N. Kumar, Phys. Rev. B802 (1975).
[14] J. N. Swingler and J. C. Inkson, J. Phys. C 10, 573 (1977).
[15] Avishav Yaniv, Phys. Rev. B 17, 3904 (1978).
[16] J. Ferrante and J. R. Smith, Solid State Commun. 20, 393 (1976).
[17] See also J. Vannimenus and H. F. Budd, Solid State Commun. 17, 1291 (1975), for a jellium-jellium interface calculation done with a gradient expansion approximation for the kinetic energy.
[18] A description of a similar calculation for the Al(111) interface by R. M. Nieminen, J. Phys. F 7, 375 (1977), appeared subsequent to Ref. 16. The self-consistency and hence the significance of the calculation is unfortunately in doubt. A check of the self-consistency is provided by the Budd-Vannimenus theorem, Ref. 19. This theorem relates the force between two jellium slabs at zero separation to properties of the uniform electron gas. The forces at zero separation given by Nieminen in his Fig. 2 for $r_s=4$ and $r_s=5$ unfortunately disagree significantly with the values -1.4×10^{-5} and 1.1×10^{-5}, respectively, given by the Budd-Vannimenus theorem.
[19] H. F. Budd and J. Vannimenus, Phys. Rev. Lett. 31, 1218 (1973).
[20] John Ferrante and J. R. Smith, Solid State Commun. 23, 527 (1977). This is a preliminary account of some of the results reported here.
[21] John Ferrante, Ph.D. thesis (Case-Western Reserve University, 1978) (unpublished).
[22] The validity of the perturbation approximation for surface energies was tested variationally by J. P. Perdew and R. Monnier, Phys. Rev. Lett. 37, 1286 (1976), (see also Ref. 23). They found it to be rather accurate for the metals tested here.
[23] R. Monnier and J.P. Perdew, Phys. Rev. B 17, 2595 (1978).
[24] N. D. Lang and W. Kohn, Phys. Rev. B 1, 4555 (1970).
[25] Monnier and Perdew (Ref. 23) found an apparent inaccuracy in the pseudopotential for Zn.
[26] N. W. Ashcroft, Phys. Rev. 155, 682 (1967).
[27] V. Heine and D. Weaire, in *Solid State Physics* (Academic, New York, 1970), Vol. 24, p. 249.
[28] D. J. Geldart and M. Rasolt, Phys. Rev. B 13, 1477 (1976); J. Shy-Yih Wang and M. Rasolt, *ibid.* 13, 5330

(1976).
[29]K. H. Lau and W. Kohn, J. Phys. Chem. Solids 37, 99 (1976). See also G. Paasch and M. Hietschold, Phys. Status Solidi 67, 743 (1975); M. Hietschold, G. Paasch, and P. Ziesche, *ibid.* 70, 653 (1975). Paasch *et al.* included gradient terms in $E_{xc}[n(\vec{r})]$ in a surface energy calculation using the gradient expansion expression for $T_s[n(\vec{r})]$ rather than Eqs. (6) and (7).
[30]J. G. Rose, Jr., H. G. Shore, D. J. W. Geldart, and M. Rasolt, Solid State Commun. 19, 619 (1976).
[31]A. K. Gupta and K. S. Singwi, Phys. Rev. B 15, 1801 (1977).
[32]J. P. Perdew, D. C. Langreth, and V. Sahni, Phys. Rev. Lett. 38, 1030 (1977) have used a wave-vector analysis rather than a gradient expansion. They obtain values for the nonlocal contribution to the exchange-correlation energy part of the jellium surface energy which are smaller than those obtained in Refs. 28–31. See also D. C. Langreth and J. P. Perdew, Phys. Rev. B 15, 2884 (1977).
[33]P. Vashishta and K. S. Singwi, Phys. Rev. B 6, 875 (1972).
[34]The authors of Ref. 28 have kindly provided us with numerical values of $C(r_s(n))$ they derived. These numerical values were fit with a simple analytic function of $r_s(n)$ to facilitate the subsequent usage of $v_{\text{eff}}[n(\vec{r});\vec{r}]$ in Eqs. (6) and (7).
[35]H. B. Huntington, Phys. Rev. 81, 1035 (1951).
[36]Norton D. Lang, Solid State Phys. 28, 296 (1973). See especially the Appendix.
[37]The asymptotic forms of the wave functions $\psi_k^{(i)}(y)$ are discussed rather completely in Ref. 11.
[38]K. H. Westmacott, R. E. Smallman, and P. S. Dobson, Mater. Sci. J. 2, 177 (1968) reported 1140 ±200 erg/cm^2 at 150–200 °C for Al.
[39]H. Wawra, Z. Metallk. 66, 395 (1975); 66, 492 (1975). Surface energies of solid metals (Al, 1169 ergs/cm^2; Zn, 1040 ergs/cm^2; and Na, 273 ergs/cm^2) are measured and extrapolated to 0 K.
[40]For Mg the experimental surface energy used is that obtained in Ref. 24 by linear extrapolation to 0 K of liquid-metal surface tensions measured by J. Bodansky and H. E. J. Shins, J. Inorg. Nucl. Chem. 30, 2331 (1968). See also W. R. Tyson and W. A. Miller, Surf. Sci. 62, 267 (1977), who list a value of 688 ergs/cm^2.
[41]For a review, see Ya. E. Geyuzin and N. N. Ovcharenko, Sov. Phys. Uspekhi 5, 129 (1962).
[42]J. E. Inglesfield, J. Phys. F 6, 687 (1976).
[43]See, e.g., Charles Kittel, *Introduction to Solid State Physics*, 3rd ed. (Wiley, New York, 1967), Chaps. 4 and 5.
[44]G. Simmons and H. Wang, *Single Crystals and Calculated Aggregate Properties* (MIT Press, Cambridge, Mass., 1971).
[45]W. R. Tyson, J. Appl. Phys. 47, 459 (1976).
[46]J. Vallin, K. Marklund, J. O. Sikström, and O. Beckman, Ark. Fys. 32, 515 (1966).
[47]G. A. Alers and J. R. Neighbours, J. Phys. Chem. Solids 7, 58 (1958).
[48]L. J. Slutsky and C. W. Garland, Phys. Rev. 107, 972 (1957).
[49]M. E. Diederich and J. Trioisonno, J. Phys. Chem. Solids 27, 637 (1966).
[50]There have been numerous calculations of elastic constants for simple (see, e.g., Refs. 51 and 52) and d-band (see, e.g., Ref. 53) metals.
[51]Duane C. Wallace, Phys. Rev. 182, 778 (1969).
[52]Walter A. Harrison, Phys. Rev. 136, A1107 (1964).
[53]U. K. Poulsen, J. Kollar, and O. K. Andersen, J. Phys. F 6, L241 (1976).
[54]M. J. Feinberg and Klaus Ruedenberg, J. Chem. Phys. 54, 1495 (1971).
[55]C. Woodrow Wilson, Jr., and William A. Goddard, III, Theoret. Chim Acta (Berl.) 26, 195 (1972).